ChemComm

COMMUNICATION

View Article Online
View Journal | View Issue

Cite this: *Chem. Commun.*, 2019, **55**, 10543

Received 18th June 2019,
Accepted 8th August 2019

DOI: 10.1039/c9cc04676c

rsc.li/chemcomm

P4T-DOTA – a lanthanide chelating tag combining a sterically highly overcrowded backbone with a reductively stable linker†

Daniel Joss and Daniel Häussinger *

Herein we report a DOTA-based lanthanide chelating tag (LCT) with rigidified backbone and a reduction-stable linker. The newly developed tag induces strong pseudocontact shifts suitable for paramagnetic protein nuclear magnetic resonance spectroscopy and the obtained anisotropic susceptibility parameters are in the range of the best performing LCTs.

Pseudocontact shifts (PCS) and residual dipolar couplings (RDC) obtained by using lanthanide chelating tags (LCT) yield valuable restraints for investigating protein structures, dynamics and interactions in solution.[1–19] The stereo-specifically methyl substituted 1,4,7,10-tetraazacyclododecane-1,4,7,10-tetraacetic acid (DOTA)-based chelators provide a sufficiently rigidified scaffold for observation of significant structural restraints.[9,20,21] Interestingly, the methyl substituents on the basic macrocyclic scaffold adopt an equatorial-upper position in the final lanthanide complex.[22,23] The methyl substituents thereby arrange in the most suitable way to provide a favourable cavity for the lanthanide ion and minimize the steric repulsion between each other. Furthermore, a crucial factor in the design of the LCTs is to obtain a lanthanide complex that shows only one diastereomer and only one conformation of the pendant arms coordinating to the lanthanide ion.[17] The conformationally locked and single diastereomeric LCT provides then only one signal set in ^{1}H–^{15}N HSQC experiments and yields strong paramagnetic effects due to its rigidity and immobilization on the proteins surface.[17] As shown by Joss *et al.*, introduction of even more bulkier isopropyl substituents on the backbone of the LCT can significantly enhance the tensor parameters when compared to its methyl substituted predecessor.[24] In order to circumvent the inherent instability of disulphide linkers towards a reductive environment, various pyridinesulphone- and iodoacetamide linkers have recently been developed. Therefore, we envisioned to synthesize a lanthanide chelating tag offering the combination of a rigidified backbone and a reductively-stable linker (Fig. 1), that enables convenient and fast protein tagging. The resulting thioether linkage is stable under reductive conditions and has been demonstrated to allow for observation of PCS and RDC in intact eukaryotic cells.[2,3]

In order to synthesize the newly designed tags, we combined the synthetic approaches by Joss *et al.* (isopropyl-substituted backbone)[24] and Müntener *et al.* (thiazolo linker)[18] and developed them further to yield the target molecule.

To explore the performance, *i.e.* the range of PCS and RDC as well as the associated $\Delta\chi$ parameters of the Ln-P4T-DOTA tag (P4T-DOTA: (2*R*,2′*R*,2″*R*)-2,2′,2″-((2*S*,5*S*,8*S*,11*S*)-2,5,8,11-tetraisopropyl-10-((2-(methylsulphonyl)thiazolo[5,4-*b*]pyridine-5-yl)methyl)-1,4,7,10-tetraazacyclododecane-1,4,7-triyl)tripropionate), the Dy-, Tm- and Lu complexes of P4T-DOTA were synthesized and conjugated to ubiquitin S57C, ubiquitin K48C and to selectively ^{15}N leucine labelled human carbonic anhydrase S166C. The newly developed LCT was benchmarked by analysing PCS and RDC (Table 1).

P4T-DOTA delivers large PCS on all tested protein constructs exceeding most current high-performance lanthanide chelating tags (Fig. 2, 3 and 5).[3,9,11,15,17,18,28,29]

The obtained tensor shapes resemble to the ones found for Ln-DOTA-M8-(4*R*4*S*)-SSPy and Ln-P4M4-DOTA, *i.e.* a significantly less rhombic tensor for the thulium complex when compared to

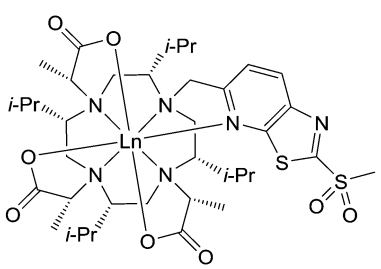

Fig. 1 Structure of Ln-P4T-DOTA in $\Lambda(\delta\delta\delta\delta)$ conformation.

Department of Chemistry, University of Basel, St. Johanns-Ring 19, 4056 Basel, Switzerland. E-mail: daniel.haeussinger@unibas.ch

† Electronic supplementary information (ESI) available. See DOI: 10.1039/c9cc04676c

Table 1 Properties of the induced axial and rhombic components of the paramagnetic susceptibility tensors ($\Delta\chi_{ax}$ and $\Delta\chi_{rh}$), metal position in PDB coordinate frame (X_{metal}, Y_{metal}, Z_{metal}), Euler angles (α, β, γ) and quality factor (Q, mathematical definition given in ESI) on ubiquitin S57C (pH 6.0), ubiquitin K48C (pH 6.0) and hCA II S166C (pH 6.8) at 298 K

Protein mutant	PDB	No. PCS	Ln^{3+}	$\Delta\chi_{ax}$ (10^{-32} m^3)	$\Delta\chi_{rh}$ (10^{-32} m^3)	X_{metal} (Å)	Y_{metal} (Å)	Z_{metal} (Å)	α (°)	β (°)	γ (°)	Q (%)
Ubiquitin S57C	1UBI[25]	50	Dy	54.0	27.0	21.6	14.5	6.0	151.7	85.5	132.4	4.5
		72	Tm	39.3	14.6	21.6	14.5	6.0	60.0	34.7	2.9	4.6
Ubiquitin K48C		32	Dy	−53.7	−23.5	20.5	19.9	25.8	117.3	117.4	118.5	21.5
		54	Tm	39.6	13.4	20.5	19.9	25.8	91.4	106.5	97.3	3.6
hCA II S166C	3KS3[26]	40	Dy	−46.1	−30.5	−15.9	−3.9	−10.8	24.4	43.7	38.9	11.4
		46	Tm	44.3	4.8	−15.9	−3.9	−10.8	174.7	157.0	29.0	5.8
Protein mutant	**PDB**	**No. RDC**	**Ln^{3+}**	**$\Delta\chi_{ax}$ (10^{-32} m^3)**	**$\Delta\chi_{rh}$ (10^{-32} m^3)**	**X_{metal} (Å)**	**Y_{metal} (Å)**	**Z_{metal} (Å)**	**α (°)**	**β (°)**	**γ (°)**	**Q (%)**
Ubiquitin S57C	2MJB[27]	24	Dy	−45.5	−26.2	15.5	−9.0	4.5	79.2	33.4	156.9	15.1
		36	Tm	−36.3	−12.3	15.5	−9.0	4.5	40.1	90.7	168.8	23.2

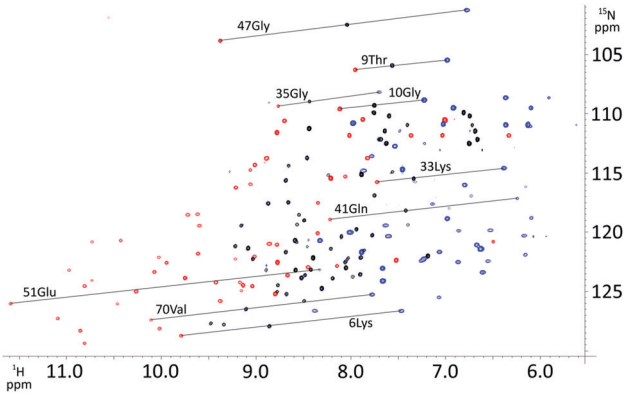

Fig. 2 Overlay of ^{1}H–^{15}N HSQC spectra of Dy- (blue), Tm- (red), and Lu-P4T-Ub^{S57C} (black).

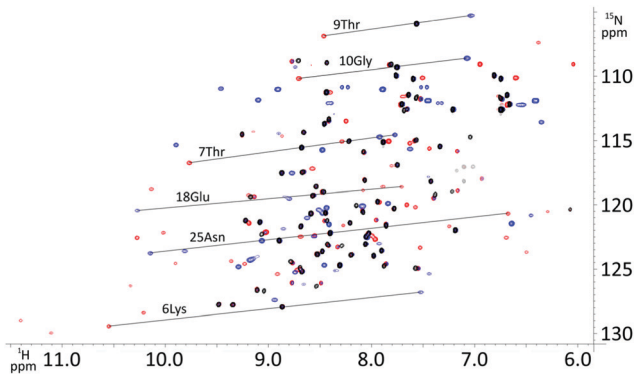

Fig. 3 Overlay of ^{1}H–^{15}N HSQC spectra of Dy- (blue), Tm- (red), and Lu-P4T-Ub^{K48C} (black).

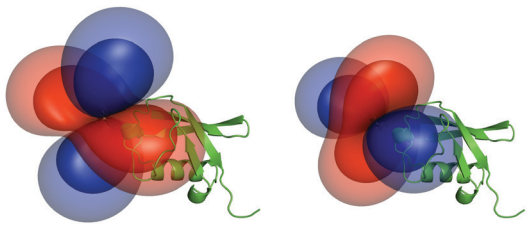

Fig. 4 Tensors generated by the dysprosium (left) and thulium (right) complex and their relative orientation to ubiquitin S57C (PCS isosurfaces set to 1.5 ppm (outer layer) and 4.0 ppm (inner layer)).

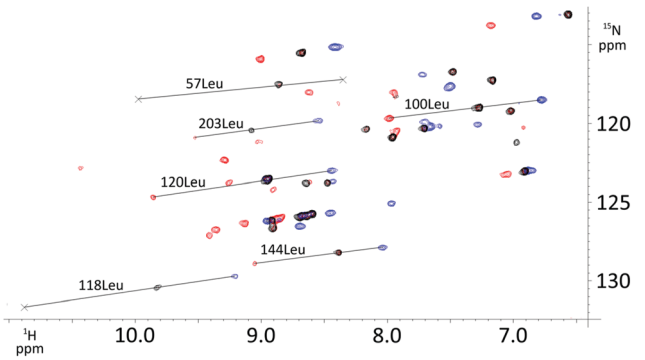

Fig. 5 Overlay of ^{1}H–^{15}N HSQC spectra of Dy- (blue), Tm- (red), and Lu-P4T (black) attached to selectively ^{15}N leucine labelled human carbonic anhydrase II S166C.

the tensor of the dysprosium complexes (Fig. 4, 6 and 7). The tensors for Tm-P4T-Ub$^{S57C/K48C}$ as well as for Tm-P4T attached to selectively ^{15}N leucine labelled hCA II S166C display a much more favourable motional averaging in comparison to Tm-DOTA-M8-(*4R4S*)-SSPy, and ensure in this way that the magnetic anisotropy of the lanthanide is efficiently transferred to the protein. This feature can be attributed to the rigid and very short thiazolo-linker, that only enables rotation around the $C_{thiazolo}$–S_{Cys} bond. Furthermore an orientation of the tag is enforced, so that the large axial lobe of the isosurfaces is colinear with the $C_{thiazolo}$–S_{Cys} bond and therefore, less diminished by rotational averaging (see Fig. 4 and 6–8).[18]

When compared to the methyl-substituted thiazolo tag described recently by Müntener *et al.*,[18] the isopropyl-substituted thiazolo tag shows an increase in tensor magnitudes due to the sterically more crowded ligand (Table 1).

Besides the favourable $\Delta\chi$-tensor properties, the reductively stable linker offers new possibilities, as *e.g.* applications in in-cell NMR, when compared to the Ln-P4M4-DOTA tag, that can only be employed under non-reductive conditions. The strong paramagnetic relaxation enhancement (PRE), *e.g.* generated for the Dy-P4T-Ub^{K48C} construct leads to relatively few detectable signals. However, the results obtained for the

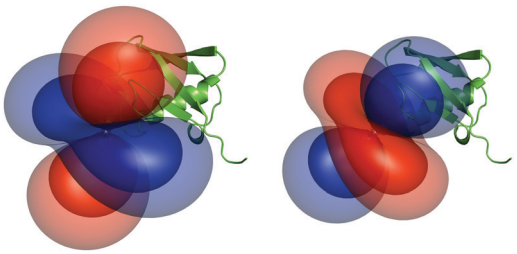

Fig. 6 Tensors generated by the dysprosium (left) and thulium (right) complex and their relative orientation to ubiquitin K48C (PCS isosurfaces set to 1.5 ppm (outer layer) and 4.0 ppm (inner layer)).

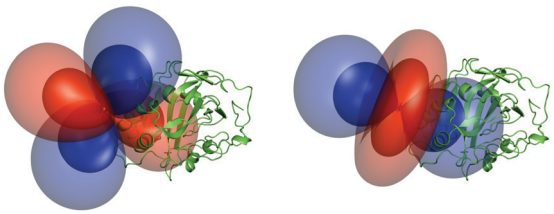

Fig. 7 Tensors generated by the dysprosium (left) and thulium (right) complex and their relative orientation to selectively ^{15}N leucine labelled hCA II (PCS isosurfaces set to 0.5 ppm (outer layer) and 2.0 ppm (inner layer)).

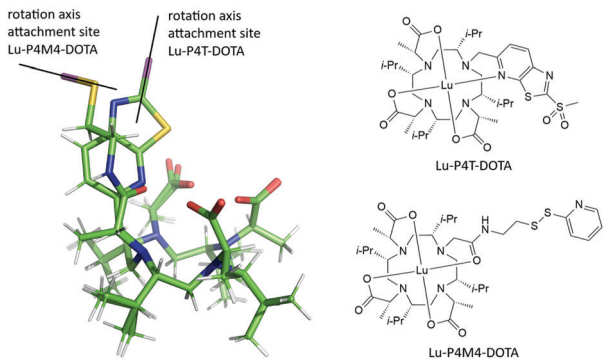

Fig. 8 Overlay of DFT structures of Lu-P4T and Lu-P4M4 and their structures. Lu-P4T (top right), Lu-P4M4 (lower right), attachment point of the protein's cysteine residue (magenta).

thulium tag when attached to ubiquitin S57C and hCA II S166C, *i.e.* the very large pseudocontact shifts combined with moderate PRE, renders the thulium P4T tag as an ideal solution to investigate not only small and medium sized proteins up to 29 kDa but shows potential for future applications to proteins with significantly larger size.

In order to further characterize the LCT presented in this study, geometries of the Lu-, Tm- and Dy complexes were calculated using density functional theory (DFT) calculations. For the calculations, BP86 was used as functional, SARC-TZVP as basis set for the ligands, while SARC2-QZVP was used as basis set for the lanthanide metal. The calculations were performed using the relativistic ZORA approximation, as well as the RI approximation to speed up the calculations. To model the water solvent, CPCM solvent model was implemented into the calculations. The corresponding references are included in the SI.

Table 2 Stabilization energies obtained *in vacuo* and water solvent (indicated as solv.). TSAP = twisted square antiprism, SAP = square antiprism

Calculated energies of the different complexes Ln(L) given in Hartree, L = P4T-DOTA		Stabilization $\Lambda(\delta\delta\delta\delta)$ (SAP) over $\Lambda(\delta\delta\delta\delta)$ (TSAP) (kJ mol^{-1})
Lu(L) TSAP	Lu(L) SAP	
−17023.78390	−17023.78679	−7.6
Lu(L) TSAP solv.	Lu(L) SAP solv.	
−17023.87054	−17023.87706	−17.1
Tm(L) TSAP	Tm(L) SAP	
−16112.77041	−16112.77262	−5.8
Tm(L) TSAP solv.	Tm(L) SAP solv.	
−16112.85311	−16112.85716	−10.6
Dy(L) TSAP	Dy(L) SAP	
−14814.69023	−14814.69733	−18.7
Dy(L) TSAP solv.	Dy(L) SAP solv.	
−14814.77349	−14814.78084	−19.3

Ln-DOTA-M8-(8*S*)-SSPy complexes show two conformational isomers depending on the ionic radius of the coordinated lanthanide, whereas the (4*R*4*S*) stereoisomer shows exclusively a $\Lambda(\delta\delta\delta\delta)$ conformation.[17,22] Based on the performed calculations with and without implicit solvent model, a clear stabilization of all investigated complexes towards a $\Lambda(\delta\delta\delta\delta)$ geometry is observed, a result that matches the outcomes for related tags (Table 2).[17,18] The obtained stabilization energies for the square antiprism (SAP) conformation of the lanthanide complexes in an implicit water solvent of 17.1 (lutetium), 10.6 (thulium) and 19.3 kJ mol^{-1} (dysprosium) correspond to equilibrium constants of 999, 73 and 2388 towards the favoured SAP conformation. Due to the higher steric demand of the thiazolo ligand close to the ninth coordination site when compared to the amide ligand of DOTA-M8-(4*R*4*S*)-SSPy and the experimental evidence by Strickland *et al.* that for the Yb-DOTA-M8-(8*S*)-SSPy with a significantly less hindered apical coordination site there is no coordination of a water molecule,[30] no calculations with an explicit water molecule on the ninth coordination site were performed.

Interestingly, from an overlay of the DFT structures of Lu-P4M4 and Lu-P4T, the angle of the LCT to the protein can be estimated (Fig. 8). Two striking differences can be observed: (i) the linker in Ln-P4T, which is rigidified by the non-flexible aromatic system, is significantly shorter and more rigid than the corresponding linker in Ln-P4M4, (ii) while Ln-P4T is attached in a favourable angle to the protein in terms of motional averaging, Ln-P4M4 is more prone to averaging of the magnetic anisotropy.

To conclude, a new, strongly paramagnetic lanthanide chelating tag is presented that yields pseudocontact shifts in a very high range, exhibits large anisotropy tensors for both employed lanthanide ions and forms a reductively stable linkage to the target protein. The newly developed tag was benchmarked on three different protein constructs, ubiquitin S57C, ubiquitin K48C and hCA II S166C. When compared to its predecessors, the presented LCT yields strongly enhanced pseudocontact shifts due to the very rigid and short linker in combination with a highly sterically crowded backbone. In order to enable further studies on large proteins, protein

complexes and other biomacromolecules by PCS NMR spectroscopy, the development of high-performance LCTs will be continued.

The Chemistry Department of the University of Basel and the Swiss National Science Foundation grant 200021_130263 are acknowledged for financial support. Biological structures were generated using the open source software PyMOL (http://www.pymol.org/). Calculations were performed at sciCORE (http://scicore.unibas.ch/) scientific computing core facility at University of Basel. C. E. Housecroft, E. C. Constable, T. Müntener and R. Vogel are acknowledged for helpful discussions.

Conflicts of interest

There are no conflicts of interest to declare.

Notes and references

1 C. Nitsche and G. Otting, *Prog. Nucl. Magn. Reson. Spectrosc.*, 2017, **98–99**, 20–49.
2 B.-B. Pan, F. Yang, Y. Ye, Q. Wu, C. Li, T. Huber and X.-C. Su, *Chem. Commun.*, 2016, **52**, 10237–10240.
3 T. Müntener, D. Häussinger, P. Selenko and F.-X. Theillet, *J. Phys. Chem. Lett.*, 2016, **7**, 2821–2825.
4 Y. Hikone, G. Hirai, M. Mishima, K. Inomata, T. Ikeya, S. Arai, M. Shirakawa, M. Sodeoka and Y. Ito, *J. Biomol. NMR*, 2016, **66**, 99–110.
5 W.-M. Liu, M. Overhand and M. Ubbink, *Coord. Chem. Rev.*, 2014, **273–274**, 2–12.
6 C. T. Loh, K. Ozawa, K. L. Tuck, N. Barlow, T. Huber, G. Otting and B. Graham, *Bioconjugate Chem.*, 2013, **24**, 260–268.
7 G. Otting, *Annu. Rev. Biophys.*, 2010, **39**, 387–405.
8 X.-C. Su, H. Liang, K. V. Loscha and G. Otting, *J. Am. Chem. Soc.*, 2009, **131**, 10352–10353.
9 D. Häussinger, J.-R. Huang and S. Grzesiek, *J. Am. Chem. Soc.*, 2009, **131**, 14761–14767.
10 X.-C. Su, B. Man, S. Beeren, H. Liang, S. Simonsen, C. Schmitz, T. Huber, B. A. Messerle and G. Otting, *J. Am. Chem. Soc.*, 2008, **130**, 10486–10487.
11 P. H. J. Keizers, A. Saragliadis, Y. Hiruma, M. Overhand and M. Ubbink, *J. Am. Chem. Soc.*, 2008, **130**, 14802–14812.
12 G. Pintacuda, A. Y. Park, M. A. Keniry, N. E. Dixon and G. Otting, *J. Am. Chem. Soc.*, 2006, **128**, 3696–3702.
13 K. D. Brewer, T. Bacaj, A. Cavalli, C. Camilloni, J. D. Swarbrick, J. Liu, A. Zhou, P. Zhou, N. Barlow, J. Xu, A. B. Seven, E. A. Prinslow, R. Voleti, D. Häussinger, A. M. J. J. Bonvin, D. R. Tomchick, M. Vendruscolo, B. Graham, T. C. Südhof and J. Rizo, *Nat. Struct. Mol. Biol.*, 2015, **22**, 555.
14 V. Gaponenko, A. S. Altieri, J. Li and R. A. Byrd, *J. Biomol. NMR*, 2002, **24**, 143–148.
15 F. Peters, M. Maestre-Martinez, A. Leonov, L. Kovacic, S. Becker, R. Boelens and C. Griesinger, *J. Biomol. NMR*, 2011, **51**, 329–337.
16 J. Wöhnert, K. J. Franz, M. Nitz, B. Imperiali and H. Schwalbe, *J. Am. Chem. Soc.*, 2003, **125**, 13338–13339.
17 D. Joss, R. M. Walliser, K. Zimmermann and D. Häussinger, *J. Biomol. NMR*, 2018, 29–38.
18 T. Müntener, J. Kottelat, A. Huber and D. Häussinger, *Bioconjugate Chem.*, 2018, **29**, 3344–3351.
19 K. Zimmermann, D. Joss, T. Müntener, E. S. Nogueira, L. Knörr, M. Schäfer, F. W. Monnard and D. Häussinger, *Chem. Sci.*, 2019, **10**, 5064–5072.
20 R. S. Ranganathan, N. Raju, H. Fan, X. Zhang, M. F. Tweedle, J. F. Desreux and V. Jacques, *Inorg. Chem.*, 2002, **41**, 6856–6866.
21 R. S. Ranganathan, R. K. Pillai, N. Raju, H. Fan, H. Nguyen, M. F. Tweedle, J. F. Desreux and V. Jacques, *Inorg. Chem.*, 2002, **41**, 6846–6855.
22 A. C. L. Opina, M. Strickland, Y.-S. Lee, N. Tjandra, R. A. Byrd, R. E. Swenson and O. Vasalatiy, *Dalton Trans.*, 2016, **45**, 4673–4687.
23 D. Parker, R. S. Dickins, H. Puschmann, C. Crossland and J. A. K. Howard, *Chem. Rev.*, 2002, **102**, 1977–2010.
24 D. Joss, M.-S. Bertrams and D. Häussinger, *Chem. – Eur. J.*, 2019, DOI: 10.1002/chem.201901692.
25 R. Ramage, J. Green, T. W. Muir, O. M. Ogunjobi, S. Love and K. Shaw, *Biochem. J.*, 1994, **299**(pt 1), 151–158.
26 B. S. Avvaru, C. U. Kim, K. H. Sippel, S. M. Gruner, M. Agbandje-McKenna, D. N. Silverman and R. McKenna, *Biochemistry*, 2010, **49**, 249–251.
27 A. S. Maltsev, A. Grishaev, J. Roche, M. Zasloff and A. Bax, *J. Am. Chem. Soc.*, 2014, **136**, 3752–3755.
28 B. Graham, C. T. Loh, J. D. Swarbrick, P. Ung, J. Shin, H. Yagi, X. Jia, S. Chhabra, N. Barlow, G. Pintacuda, T. Huber and G. Otting, *Bioconjugate Chem.*, 2011, **22**, 2118–2125.
29 F. Yang, X. Wang, B.-B. Pan and X.-C. Su, *Chem. Commun.*, 2016, **52**, 11535–11538.
30 M. Strickland, C. D. Schwieters, C. Göbl, A. C. L. Opina, M.-P. Strub, R. E. Swenson, O. Vasalatiy and N. Tjandra, *J. Biomol. NMR*, 2016, **66**, 125–139.

